



Is the cloud absorption of solar radiation still underestimated notably by current model-based reanalyses?

You-Jing FU^{a,b}, Guang-Hui HUANG^{a,b,*}, Zi-Yan HUANG^{a,b}, Xu-Feng WANG^{c,d},
Han MA^{e,f}, Guo-Jiang WANG^{a,b}, Chun-Lin HUANG^{c,d}, Xiao-Hua HAO^{c,d},
Peng-Fei ZHAO^{a,b}

^a College of Earth and Environmental Sciences, Lanzhou University, Lanzhou 730000, China

^b Center for Remote Sensing of Ecological Environments in Cold and Arid Regions, Lanzhou University, Lanzhou 730000, China

^c Key Laboratory of Remote Sensing of Gansu Province, Northwest Institute of Eco-Environment and Resources, Chinese Academy of Sciences, Lanzhou 730000, China

^d Heihe Remote Sensing Experimental Research Station, Northwest Institute of Eco-Environment and Resources, Chinese Academy of Sciences, Lanzhou 730000, China

^e JC STEM Lab of Quantitative Remote Sensing, Department of Geography, The University of Hong Kong, Hong Kong 999077, China

^f International Center for China Development Studies, The University of Hong Kong, Hong Kong 999077, China

Received 25 April 2025; revised 28 September 2025; accepted 16 October 2025

Available online 23 October 2025

Abstract

Cloud absorption of solar radiation strongly influences Earth's radiation balance and climate change. Whether numerical models underestimate this absorption compared with observations has long been a highly debated issue in cloud–radiation research. Using state-of-the-art model-derived reanalyses, NCEP CFSv2, ECMWF ERA5, and NASA MERRA2, and the latest collocated satellite-surface observation in 2012–2023, we reinvestigate this controversial issue. The results demonstrate the observed cloud absorption of solar radiation still notably exceeds the modeled (regardless of model products), but their discrepancy has dropped a lot, particularly for NCEP CFSv2 and ECMWF ERA5. While a further investigation is needed, the reduced discrepancy may reflect the progress of shortwave radiation schemes in models, notably the integration of Rapid Radiative Transfer Model for General Circulation Models (RRTMG) and the Monte Carlo Independent Column Approximation (McICA). Additionally, it is noteworthy that there is not a perfect approach to obtaining the observed cloud absorption, and particularly the water vapor difference between clear and cloudy skies will often result in its unrealistic overestimation. If the impact from the water vapor difference is corrected, NCEP CFSv2, ECMWF ERA5, and NASA MERRA2 underestimate globally-mean cloud absorption by approximately 8.26, 14.50 and 16.51 W/m², respectively.

Keywords: Solar radiation; Clouds; Numerical models; Atmospheric absorption; Shortwave radiation schemes

* Corresponding author. College of Earth and Environmental Sciences, Lanzhou University, Lanzhou 730000, China.

E-mail address: huanggh@lzu.edu.cn (HUANG G.-H.).

Peer review under responsibility of National Climate Centre (China Meteorological Administration)

1. Introduction

Clouds are the largest moderator of Earth's radiation budget, and their absorption of solar radiation directly influences our understanding of climate change

(Hausfather et al., 2022). Cloud absorption anomaly refers to the phenomenon that observed cloud-absorbing solar radiation from collocated satellite (or aircraft) and surface measurements, often notably exceeds the theoretical calculation by models (Huang et al., 2019; Li et al., 1997; Pincus et al., 2003). Since solar radiation absorbed by the Earth and atmosphere is the fundamental driving forces of dynamical, hydrological, and thermal processes in our climate system, this systematic discrepancy (or bias) may heavily hinder our modeling or projection on climate change through models (Feng et al., 2025; He et al., 2025; Kiehl et al., 1995; Zhao et al., 2025).

There has been a long history of the alleged cloud absorption anomaly that is not explained clearly. Questions about whether it really exists, how much it is, and what are underlying causes, ever raised widespread concern and also great controversy in the mid-1990s. All these were sparked by three companion studies, in which Ramanathan et al. (1995), Cess et al. (1995) and Pilewskie and Valero (1995) thought anomalous absorption of solar radiation by clouds was not only universal but also much larger than previously believed. While some closely following studies (Li et al., 1995; Stephens, 1996) highlighted certain shortcomings in these studies, the more studies reinforced their conclusion (Ackerman and Toon, 1996; Arking, 1996; Wiscombe, 1995) and proposed various reasons to explain the phenomenon. One popular reason given at that time was there might be systematic observation errors (Haeffelin et al., 2001; Satheesh and Ramanathan, 2000) due to imprecise radiation calibration of pyranometers and satellite sensors in the 1980s and 1990s (especially thermal offset errors of pyranometers), whereas other studies (Arking, 1996; Crisp, 1997; Li et al., 1997) attributed it to the problem of models themselves and thought radiative transfer schemes in then general circulation models (GCMs) oversimplified or missed certain physical processes.

At almost the same time, long-term surface radiation observation programs with higher accuracy such as the Baseline Surface Radiation Network (BSRN) and the Atmospheric Radiation Measurement (ARM), had been initiated in an attempt to enhance the understanding of cloud–radiation interactions, and subsequently help model developers refine cloud shortwave radiative transfer codes (Ohmura et al., 1998; Stokes and Schwartz, 2003). As anticipated, the utilization of these updated observations led to the emergence of different viewpoints in the early 2000s. For instance, several ARM studies (Ackerman et al., 2003; Asano et al., 2004; Li et al., 2002; O’Hirok and Gautier, 2003) refuted the existence of the cloud absorption anomaly, attributing it primarily to sampling issues, inhomogeneity of cloud fields and the surface, or known uncertainties in observations and model inputs.

The heated dispute, however, appears to have subsided over time. Over the past two decades, both GCMs (or later coupled models) and satellite/surface observations have undergone steady improvements (Hogan and Bozzo, 2018;

Molod et al., 2015; Morcrette et al., 2008). Especially since 2000, reanalysis products obtained through models and data assimilation have gained widespread application. The reanalysis process assimilates diverse observations to generate an initial analysis field, which is then input into models to produce a globally gridded, physically consistent, long-term climate dataset (Fang and Cao, 2025; McFarlane et al., 2016; Saha et al., 2014). Through data assimilation, reanalysis improves the traditionally low simulation accuracy of clouds in models while preserving the integrity of cloud–radiation physical processes (variables related to radiation fluxes are non-state variables and are generally referred to as derived variables or model output variables). Naturally, we are interested in whether a systematic discrepancy still exists between current model-derived reanalyses and observations. Therefore, in this study, we reinvestigate these discrepancies using three state-of-the-art model-derived reanalyses and the latest observations from satellites and the surface, then discuss the uncertainties, and finally again quantify the magnitude of the so-called ‘cloud absorption anomaly’.

2. Data and method

2.1. Observation data

Radiative flux observations at the top of the atmosphere (TOA) are derived from the Terra/Aqua Clouds and the Earth’s Radiant Energy System (CERES) Level 2 Single Scanner Footprint (SSF) products (<https://ceres.larc.nasa.gov>), while surface flux observations are sourced from two well-maintained measurement networks (Table A1, over land 27 sites and over ocean 2 sites): the World Climate Research Programme (WCRP) Baseline Surface Radiation Network (BSRN, <https://bsrn.awi.de>) and the National Oceanic and Atmospheric Administration (NOAA) Surface Radiation Budget Network (SURFRAD, <https://gml.noaa.gov>). The Terra/Aqua CERES is a broadband radiometer with a nadir footprint size of 20 km, capable of reducing systematic observation errors in TOA fluxes by a factor of 2–4 compared to its predecessor, the Earth Radiation Budget Experiment (ERBE) (Su et al., 2015). The WCRP-BSRN is a global surface radiation observation network sponsored by the World Meteorological Organization, designed to provide uniform, continuous, and benchmark-quality shortwave and longwave radiation measurements for climate research. The NOAA-SURFRAD, a regional observing network, is established, operated, and calibrated in accordance with BSRN specifications. WCRP-BSRN and NOAA-SURFRAD both provide reference-grade surface radiation measurements and the uncertainty of solar radiation is generally within several W/m^2 .

In addition to the aforementioned flux observations, this study also uses two Moderate-Resolution Imaging Spectroradiometer (MODIS) products (<https://search.earthdata.nasa.gov>): CERES synchronous MODIS cloud

mask products, and the daily MODIS albedo product. The synchronous MODIS cloud mask product provides detailed fractional cloud cover data for each CERES footprint, enabling accurate identification of clear and cloudy samples. Meanwhile, the high-resolution MODIS albedo product is used to derive surface albedo at the same spatial resolution as CERES footprints, thereby addressing the impact of surface inhomogeneity on radiative flux closure (Li et al., 2002). Basic information of all observed data is listed in Table 1.

2.2. Modeled data

The modeled data comes from three widely-used hourly reanalyses: the National Centers for Environmental Prediction (NCEP) Climate Forecast System Version 2 (CFSv2) (<https://rda.ucar.edu/>), the European Centre for Medium-Range Weather Forecasts (ECMWF) ERA5 (<https://cds.climate.copernicus.eu>), and the National Aeronautics and Space Administration (NASA) Modern-Era Retrospective analysis for Research and Applications 2 (MERRA2) (<https://gmao.gsfc.nasa.gov>). Table 2 lists the basic information of these model products.

It is noteworthy that it seems that the shortwave radiation schemes in NCEP CFSv2 and ECMWF IFS are similar and more advanced than that in GMAO GEOS5. NCEP CFSv2 and ECMWF IFS introduce the newest Rapid Radiative Transfer Model (RRTM) for GCMs (Hogan and Bozzo, 2018; Saha et al., 2014) and the Monte Carlo Independent Column Approximation (McICA) (Pincus et al., 2003) to improve their cloud–radiation interaction schemes. GMAO GEOS5 (Molod et al., 2015), however, still adopted the conventional codes of Chou and Suarez (1999).

Table 1
Basic information of surface and satellite observations used.

Observation	Spatial resolution	Time resolution	Observed parameter
BSRN/SURFRAD	Site-specific	1 min ^a	Surface incident shortwave flux
CERES SSF	20 km × 20 km	Instantaneous	TOA upward shortwave flux
CLDPROP (MODIS)	1 km × 1 km	Instantaneous	Cloud area fraction
MCD43A3 (MODIS)	500 m × 500 m	Daily	Surface albedo (white-sky albedo)

Note: ^aTo improve the spatial representativeness of ground-based observation, a 30-min (±15 min) temporal smoothing (Huang et al., 2016) was applied to BSRN/SURFRAD surface incident solar radiation measurements.

Table 2
Basic information of three model products.

Model product	Horizontal resolution	Time resolution	Temporal coverage	Climate model	Radiation scheme
NCEP CFSv2	0.205° × 0.204°	1-h	2011–present	NCEP climate forecast system (CFS)	RRTMG ^a + McICA ^b
ECMWF ERA5	0.25° × 0.25°	1-h	1979–present	ECMWF integrated forecast system (IFS)	RRTMG + McICA
NASA MERRA2	0.625° × 0.5°	1-h	1980–present	Goddard earth observing system model version 5 (GEOS5)	Chou and suarez ^c

Note: ^aRRTMG, Rapid Radiative Transfer Model for General Circulation Models; ^bMcICA, Monte Carlo Independent Column Approximation; ^cAlthough the newest GEOS5 already introduced the RRTMG and McICA (Norris et al., 2020), current NASA MERRA products are still produced utilizing the code of Chou and Suarez (1999).

All observed and modeled data from 2012 to 2023 will be meticulously selected to form the samples. To reduce the impact of cloud field inhomogeneity, only entirely clear and overcast cases will be considered. To minimize the influence of observational errors, all observations undergo rigorous screening and cases involving precipitation, dust, or snow are excluded.

2.3. Methods

Following the previous studies (Cess et al., 1995; Li and Moreau, 1996; Li and Trishchenko, 2001), we first adopt a ratio, R , to determine the discrepancy of cloud absorption between observation and modeling. It is defined as,

$$R = \text{CRF}_{\text{SUR}} / \text{CRF}_{\text{TOA}} \quad (1)$$

where CRF_{SUR} and CRF_{TOA} are shortwave cloud radiative forcing (CRF) at surface and TOA, respectively. Thereby, the atmospheric CRF, CRF_{ATM} , is,

$$\text{CRF}_{\text{ATM}} = \text{CRF}_{\text{TOA}} - \text{CRF}_{\text{SUR}} = (1 - R)\text{CRF}_{\text{TOA}} \quad (2)$$

Generally $\text{CRF}_{\text{TOA}} < 0$, therefore, $R > 1$, $R = 1$, and $R < 1$ imply the enhanced, unchanged, and reduced atmospheric absorption caused by clouds relative to clear skies, respectively.

Supposing that the absorptions by the other atmospheric constituents (*e.g.*, water vapor, aerosols, ozone, gases) remain constant between cloudy and clear skies, CRF_{ATM} , namely atmospheric CRF, can be approximated as cloud-induced absorption. Therefore, the R -value indicates the magnitude of cloud absorption.

Because R is not a direct absorption representation after all, here we also introduce another more straightforward parameter, absorptivity, to discuss atmospheric absorption

and cloud absorption. It is defined as the percentage (%) of solar radiation absorbed by atmosphere relative to TOA incident radiation. Under the same assumption, the cloud-induced absorptivity, α_c , can be approximated to,

$$\alpha_c \approx \alpha_{ca} - \alpha_{sa} \tag{3}$$

where α_{ca} denotes the absorptivity of cloudy atmospheres, and α_{sa} denotes that of clear (or sunny) atmospheres.

It should be noted that the observed R and α_c are calculated on the basis of the monthly collocated satellite and surface observation, whereas the modeled R and α_c are computed according to the modeled cloudy-sky samples and their corresponding cloudless modeling. Furthermore, the paired samples t -test (Ross and Willson, 2018) will be used to examine the significance of their discrepancy that one modeled cloud absorption is lower than the observed.

3. Results

3.1. Discrepancy between NCEP CFSv2 and the observation

First, let us focus on the overall comparison, where all available samples from BSRN/SURFRAD sites are taken into account together. Fig. 1 gives the distributions of the NCEP CFSv2 modeled R , the observed R , the modeled α_c (cloud absorptivity) and the observed α_c obtained at all sites. NCEP CFSv2 modeled R values are predominantly clustered within the narrow range of 0.90–1.32, whereas observed R values fluctuate significantly from 0.59 to 1.80. The mean R for NCEP CFSv2 is 1.11, whereas the observed mean R is 1.19. Comparing against the observation, the R bias given by NCEP CFSv2 is -0.08 . As a whole the NCEP CFSv2 modeled R is clearly less than the observed R .

A similar but clearer feature can be seen for α_c . The mean α_c for NCEP CFSv2 is 3.88%, while the mean α_c revealed by the observation is as high as 6.65%. The NCEP CFSv2 modeled mean cloud absorptivity is approximately half of the observed. The bias of NCEP CFSv2 α_c is up to -2.27% . The t -test for all α_c sample pairs of NCEP CFSv2 and the observation also supports that NCEP CFSv2 underestimates cloud absorption significantly. Therefore, cloud absorption is overall still underestimated by NCEP CFSv2, no matter from the R perspective or from the α_c perspective.

Fig. 2 further gives site-by-site comparisons, in which shown on the top is the NCEP CFSv2 modeled site-averaged R value versus the observed at every BSRN/SURFRAD site and on the bottom is the corresponding α_c comparing. We can see that the modeled site-averaged R values are concentrated in the interval of 1.08–1.25, versus 1.07–1.45 of the observed. At most sites (22 out of 29, marked by red circles in Fig. 2) modeled R values are significantly lower than the observed (noticeably negative biases). Only at TBL, DRA, PSU, TOR, PAY, DAR, and TAT (Table A2) are the modeled R values slightly higher than or equal to the observed.

The comparison of α_c (shown at the bottom of Fig. 2) displays similar but some different results. NCEP CFSv2 modeled site-averaged α_c values are 2.30%–7.28%, whereas corresponding observed α_c values are 2.54%–10.84%. At 26 sites (total 29 sites) the observed values are higher (negative biases), although at DRA, PSU and DAR their discrepancies are statistically insignificant (marked by green circles in Fig. 2). At many sites (15 out of 29) the observed α_c values are even more than twice as large as the modeled values. Only at PAY, TOR, and TAT are the observed values lower than the NCEP CFSv2 modeled values. It is surprising that a distinct result is found at TBL.

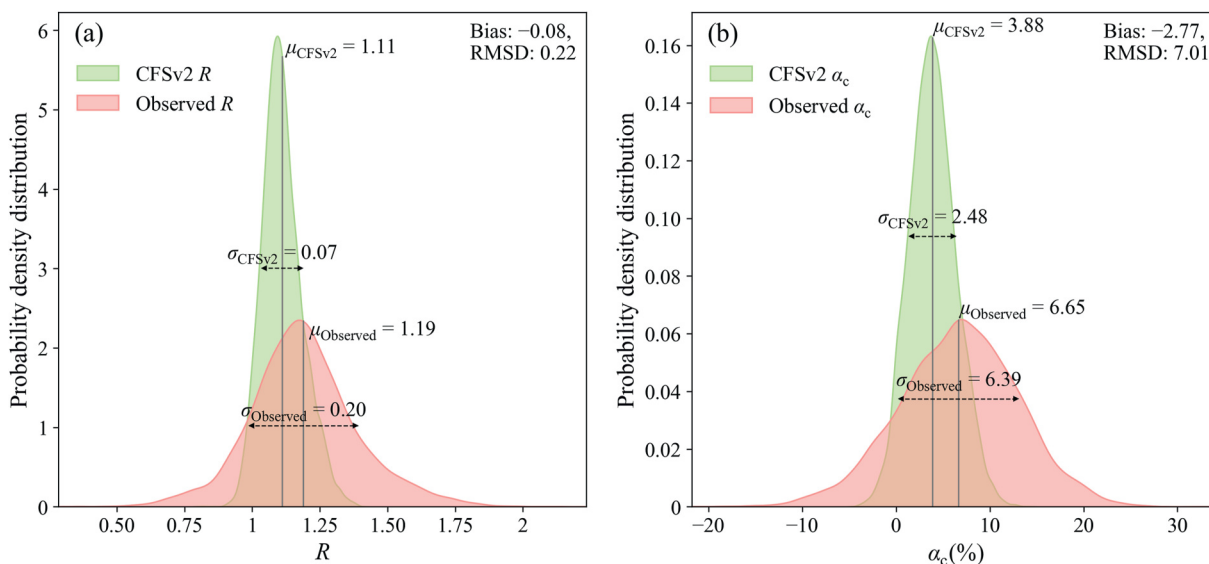


Fig. 1. Distributions of (a) R and (b) α_c values obtained at all sites: NCEP CFSv2 versus the observation (μ denotes the mean, and σ denotes one standard deviation).

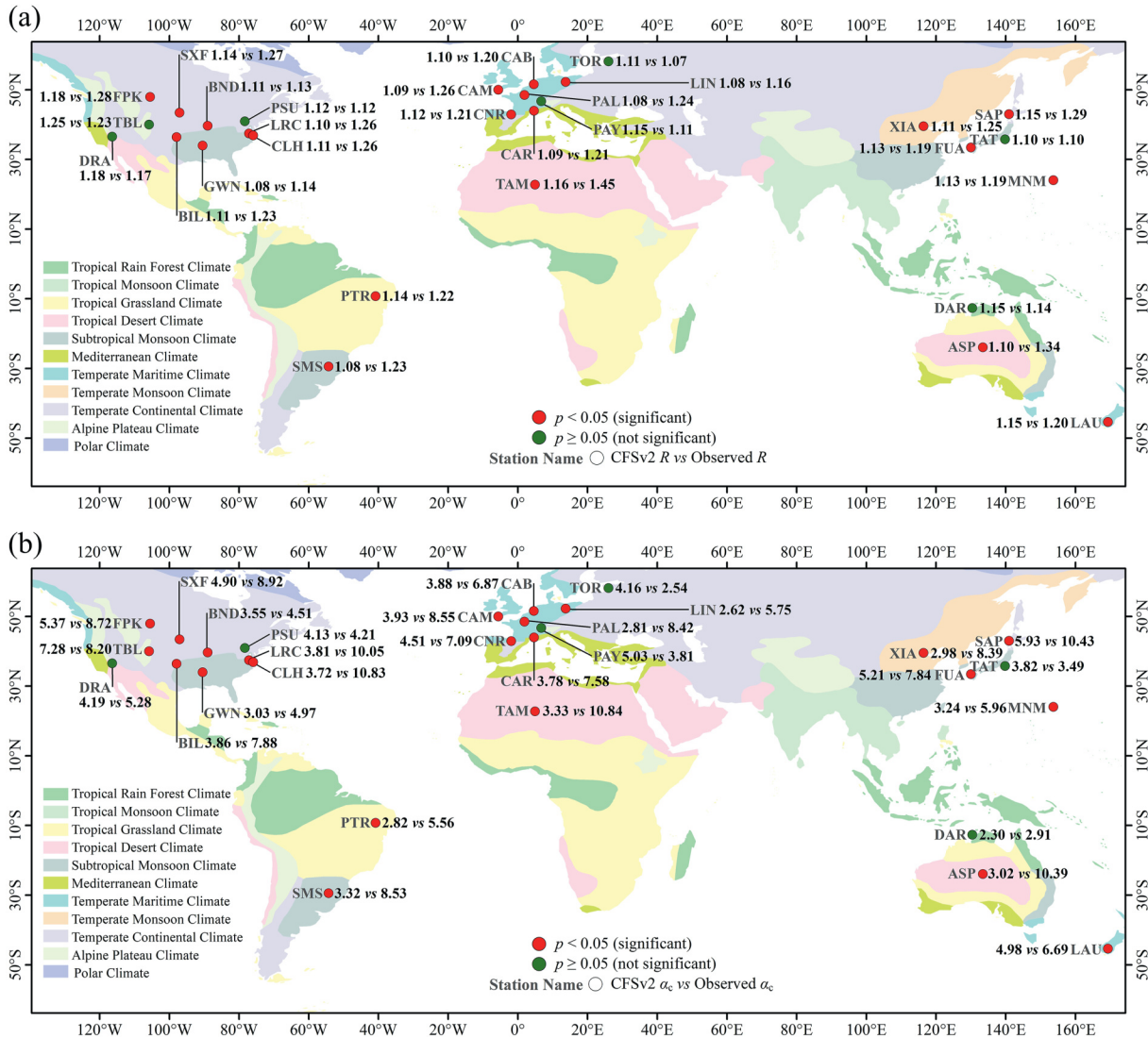


Fig. 2. Difference of the site-averaged (a) R and (b) α_c at each BSRN or SURFRAD site between NECP CFSv2 and its corresponding observation.

From the R point of view the cloud absorption is slightly overestimated by NCEP CFSv2 as mentioned before, but from α_c point of view it is significantly underestimated. These differences may result from one of the R drawbacks, as its calculation is more sensitive to the accuracy of surface albedo (Li et al., 2002).

Therefore, site-by-site comparisons demonstrate the cloud absorption is still underestimated by NCEP CFSv2 at most sites and this underestimation is frequently statistically significant (red circles in Fig. 2).

3.2. Discrepancy between ECMWF ERA5 and the observation

Accordingly, Fig. 3 gives the overall comparison between ECMWF ERA5 and the observation using all available samples. We can see that ECMWF ERA5 modeled R values are clustered within the narrow range of 0.86–1.28, in contrast, observed R values still fluctuate

drastically from 0.54 to 1.86. The ECMWF ERA5 mean R is 1.07, while the observed mean R is up to 1.20. Comparing against the observation, the bias of ECMWF ERA5 R is -0.12 . As a whole the ECMWF ERA5 modeled R is remarkably less than the observed, too.

Let us look at the other more direct parameter, α_c . The ECMWF ERA5 mean α_c is only 1.85%, but the mean α_c revealed by the observation is as high as 6.36%. The ECMWF ERA5 modeled mean cloud absorptivity is less than one third of the observed. Comparing against the observation, the bias of ECMWF ERA5 α_c is -4.51% . The paired samples t -tests for R and α_c both indicate the discrepancy is significant that the ECMWF ERA5 modeled cloud absorption is less than the observed.

Fig. 4 provides more detailed site-by-site comparisons. We can see the maximum R from the observation can be up to 1.40 at TAM, while the maximum R from ECMWF ERA5 is only 1.22 also at TAM. At all sites, ECMWF ERA5 modeled site-averaged R values are uniformly less

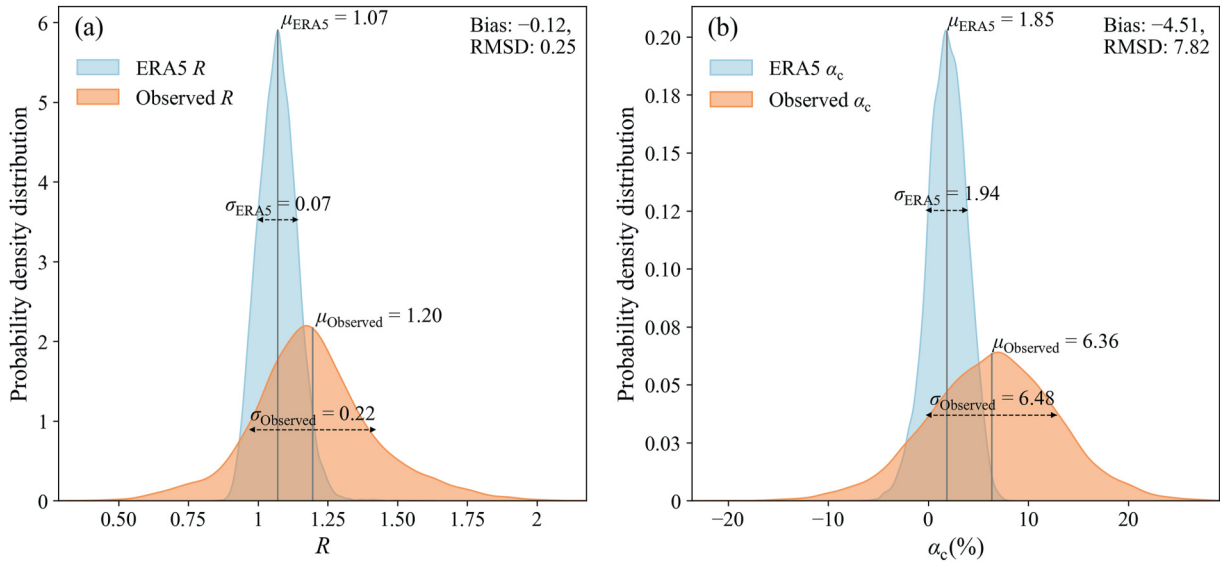


Fig. 3. Distributions of (a) R and (b) α_c values obtained at all sites: ECMWF ERA5 versus the observation (μ denotes the mean, and σ denotes one standard deviation).

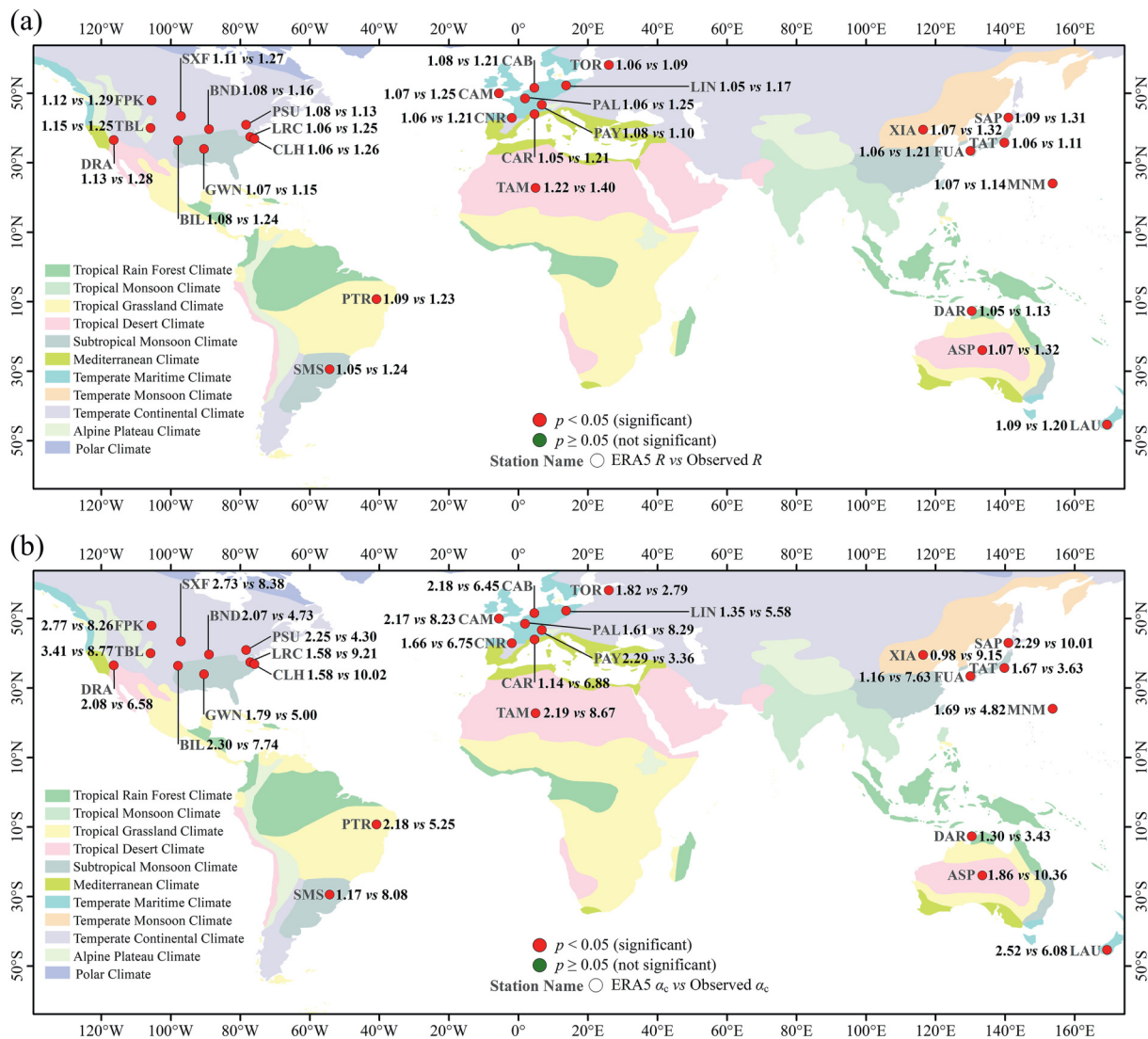


Fig. 4. Difference of the site-averaged (a) R and (b) α_c at each BSRN or SURFRAD site between ECMWF ERA5 and its corresponding observation.

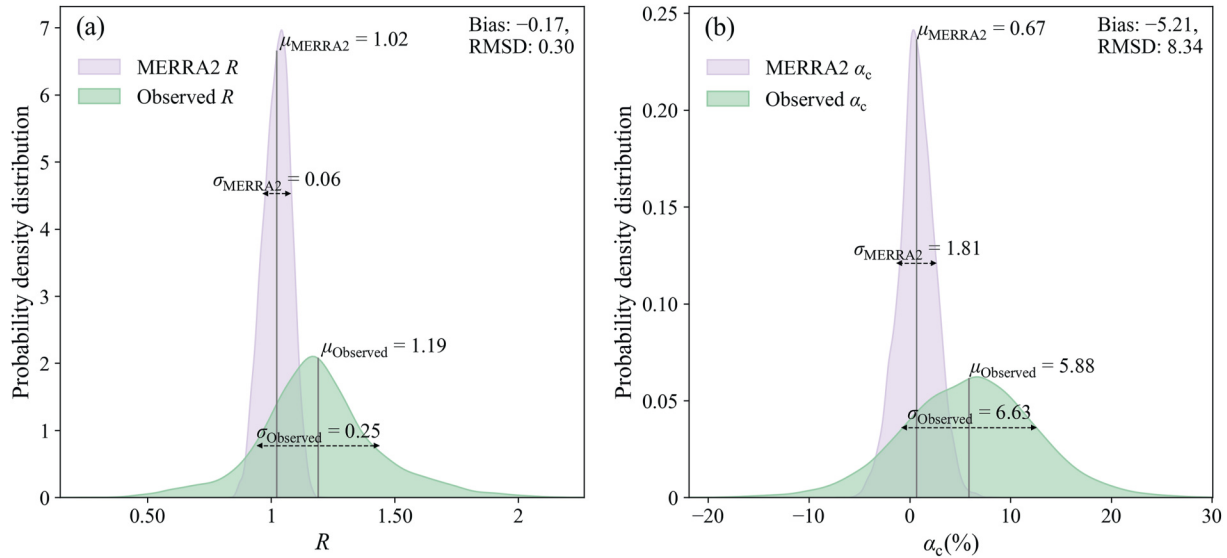


Fig. 5. Distributions of (a) R and (b) α_c values obtained at all sites: NASA MERRA2 versus the observation (μ denotes the mean, and σ denotes one standard deviation).

than the observed and their discrepancies are all statistically significant (Fig. 4).

The site-by-site α_c comparisons reinforce the same conclusion. Among all 29 sites, there are as many as 14 sites where ECMWF ERA5 modeled α_c values are even less than one third of the observed, 12 sites where modeled α_c values are between one third and one half of the observed, and only 3 sites at which modeled α_c values are larger than one half of the observed. The relatively smallest discrepancy happens PAY, where ECMWF ERA5 modeled α_c can be up to 68% of the observed, whereas the largest discrepancy happens at XIA, where ECMWF ERA5 modeled α_c is only 11% of the observed. The site-specific biases range from -0.97% to -8.50% (Table A2).

Therefore, both the overall comparison and site-by-site comparisons demonstrate cloud absorption is still notably underestimated by ECMWF ERA5 and its discrepancy with the observation is larger than that of NCEP CFSv2.

3.3. Discrepancy between NASA MERRA2 and the observation

The overall comparison between NASA MERRA2 and the observation is presented in Fig. 5. It can be seen that the mean R of NASA MERRA2 is 1.02, compared to 1.19 for the observation. The mean α_c of NASA MERRA2 is only 0.67%, compared to 5.88% for the observation. Comparing against the observation, the biases of R and α_c are -0.17 and -5.21% , respectively. No matter from the R or α_c perspective, cloud absorption is underestimated by NASA MERRA2 heavily. Of course, the paired samples t -tests for R and α_c both support that the underestimation of NASA MERRA2 is statistically significant ($p < 0.01$).

Let us now turn our attention to the parameter, α_c . As shown in the right panel of Fig. 5, the peak value of α_c

modeled by NASA MERRA2 is approximately 0.34% (even lower than the mean), suggesting that cloud absorption in NASA MERRA2 is in fact very minimal. In any case, the modeled α_c value does not exceed 6.08%. In contrast, the observed α_c peak value reaches approximately 6.15%. The maximum α_c value provided by NASA MERRA2 remains lower than the observed α_c peak value. The mean α_c value provided by NASA MERRA2 is only about 11% of the observed.

Detailed comparisons at each BSRN and SURFRAD site are illustrated by Fig. 6. One can see the site-averaged R values from NASA MERRA2 remain relatively constant across sites, with the maximum R reaching only 1.07 (at MNM in the Western Pacific). In contrast, the observed site-averaged R values fluctuate dramatically, with the minimum R reaching 1.08 (at TOR in Northern Europe). The site-specific biases range from -0.06 to -0.18 (Table A2). At each site, cloud absorption is consistently underestimated by NASA MERRA2, and the underestimations is significant.

A similar conclusion can be drawn from the perspective of α_c . In fact, at most sites (19 out of 29) averaged cloud absorptivity given by NASA MERRA2 are less than 1%. Even at LIN, XIA, and MNM (Table A2), the modeled average cloud absorptivity approaches zero (or is even lower), suggesting that in the NASA MERRA2 model, the presence of clouds does not lead to increased absorption of solar radiation at these sites. At 25 out of the 29 sites, the modeled α_c values are less than one-quarter of the observed values, with the smallest discrepancy occurring at TAT, where the NASA MERRA2 modeled α_c reaches only 38% of the observed value.

Combining Figs. 1, 3 and 5, we can conclude that overall NASA MERRA2 most significantly underestimates cloud absorption, followed by ECMWF ERA5, with NCEP

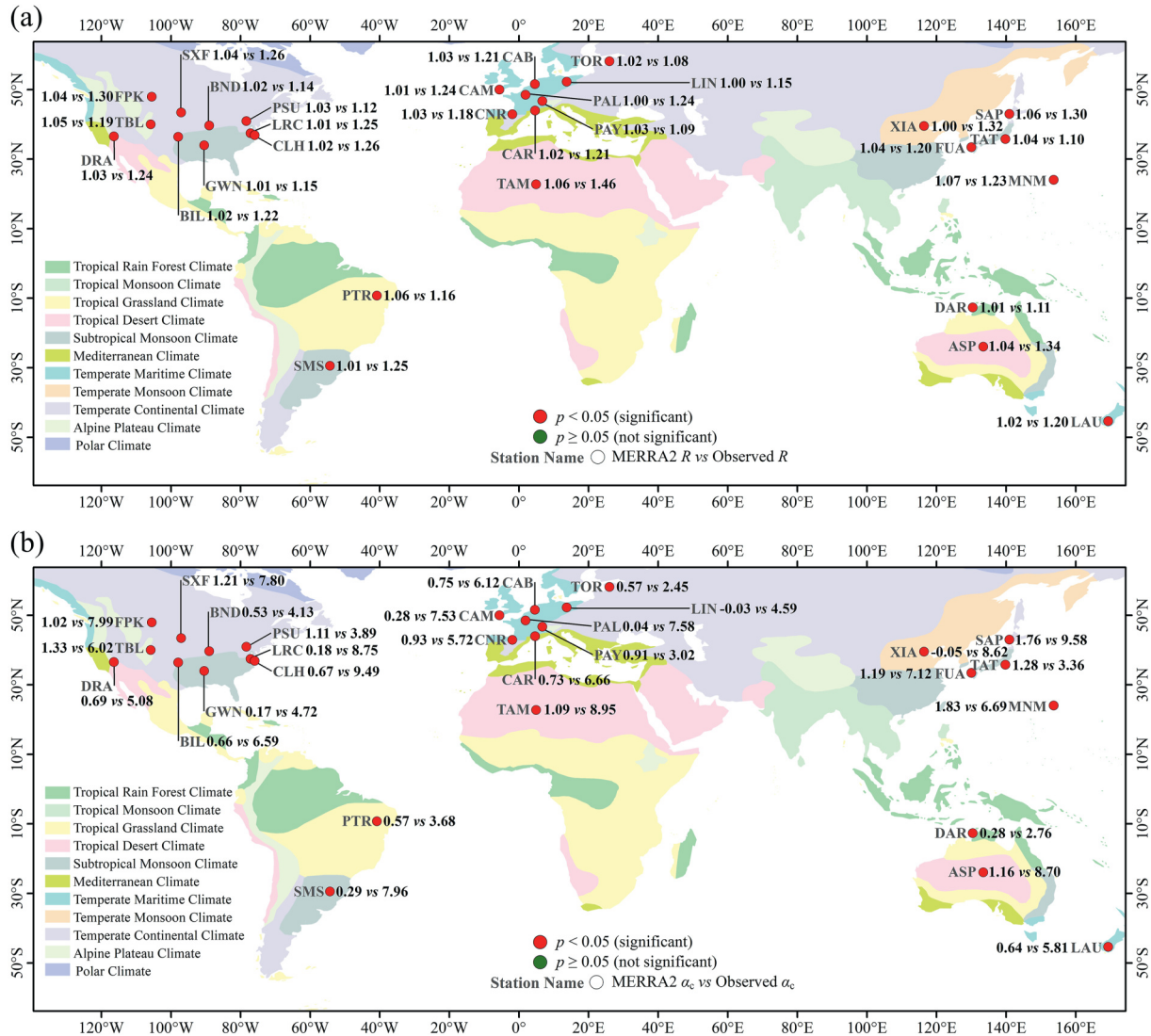


Fig. 6. Difference of the site-averaged (a) R and (b) α_c at each BSRN or SURFRAD site between NASA MERRA2 and its corresponding observation.

CFSv2 exhibiting the smallest underestimation. Combining Figs. 2, 4 and 6, we can conclude that the underestimation of cloud absorption by NCEP CFSv2 is significant at most sites, while the underestimations by ECMWF ERA5 and NASA MERRA2 are significant across all sites.

4. Discussion

4.1. Limitations of the observation

We must point out that the modeled R and α_c do represent cloud-induced absorption, but strictly speaking, the observed cannot because here we need an assumption that absorptions from the other atmospheric constituents except clouds should be consistent between cloudy and clear skies. This assumption is questionable, particularly for water vapor, as water vapor concentrations in cloudy atmospheres are often higher than in clear skies (Crisp, 1997). Therefore, in this section we choose 10 sites that have

supplementary near-surface temperature and humidity observations to examine the impact of the water vapor difference between clear and cloudy skies on the observed and R and α_c .

First, column water vapor is estimated from observed near-surface relative humidity and temperature using a semi-empirical formula by Yang et al. (2006), while water vapor transmittance is calculated through the representative wavelengths absorption parameterization approach provided by the libRadtran (Emde et al., 2016). Subsequently, surface radiation observations under clear skies are adjusted based on the difference in column water vapor between clear and cloudy skies. Finally, based on these adjusted clear-skies observation, the new observed R and α_c values are recomputed.

Table 3 lists the changes in the observed R and α_c after this adjustment. We find compared with the raw, the new R and α_c do drop a bit, which indicates partially excessive cloud absorption from the observation is indeed resulted

Table 3
Observed site-averaged R and α_c values before and after the water vapor adjustments at 10 BSRN/SURFRAD sites.

Site	Observed R			Observed α_c (%)		
	Raw	New	ΔR	Raw	New	$\Delta \alpha_c$
BND	1.16	1.13	-0.03	4.8	4.0	-0.8
CAB	1.21	1.20	-0.01	6.2	5.9	-0.3
CAR	1.20	1.18	-0.02	6.2	5.6	-0.6
CNR	1.20	1.18	-0.02	6.1	5.5	-0.6
FPK	1.29	1.27	-0.02	8.1	7.5	-0.6
LIN	1.14	1.12	-0.02	4.8	4.0	-0.8
PAL	1.25	1.22	-0.03	7.9	7.0	-0.9
PSU	1.16	1.13	-0.03	4.6	4.0	-0.6
SXF	1.26	1.24	-0.02	7.9	7.3	-0.6
TBL	1.23	1.19	-0.04	7.6	6.7	-0.9

Note: Here the listed R or α_c values are specific to all available observed samples at each site, they have slight differences with those shown in Figs. 2, 4 and 6.

from cloudy-sky higher water vapor content. However, the reductions in R caused by the water vapor difference are only 0.01–0.04, while the decreases in α_c are only 0.3%–0.9%. Even when its influence is accounted for, the results presented in Section 3 do not undergo significant changes.

Besides water vapor, other observational limitations may also undermine our results. These limitations include insufficient spatial representativeness of surface sites, aerosol difference between clear skies and cloudy skies, observation errors, *etc.* But we do not think they will alter our results substantially.

4.2. Absorptivity of cloudy atmospheres: reanalyses versus observation

Given the inherent sensitivity of the observed R and α_c values to clear-sky measurements, this section directly compares atmospheric absorptivity under cloudy skies (α_{ca}) between reanalyses and the observation.

Box-and-whisker plots in Fig. 7 illustrate the distributions of α_{ca} derived from the observation, NCEP CFSv2, ECMWF ERA5 and NASA MERRA2 across all BSRN/SURFRAD sites. As expected, the observed atmospheric absorptivity for cloudy skies notably exceeds those predicted by the three reanalyses at nearly all sites (except DRA in the American West). Only at DRA the observed mean α_{ca} is slightly lower than the NCEP CFSv2 modeled. The observed site-averaged α_{ca} values fluctuate between 24% and 32%, while the NCEP CFSv2, ECMWF ERA5, and NASA MERRA2 model values range 24%–27%, 21%–27%, and 18%–24%, respectively. Similarly, NCEP CFSv2 agrees most closely with the observations, followed by ECMWF ERA5. The discrepancy between NASA MERRA2 and the observations is so large that at many sites all model values fall below the observed means, further indicating that the radiation scheme currently used by NASA MERRA2 may require improvement (Norris et al., 2020).

Table A3 gives more detailed statistics on validations of α_{ca} for the three model products. Depending on the sites,

the biases of NCEP CFSv2 range from -0.43% to -4.39% (excluding DRA), those of ECMWF ERA5 range from -0.50% to -4.62%, and those of NASA MERRA2 range from -3.16% to -7.82%. Negative biases at nearly all sites (excluding DRA) also reveal that atmospheric absorption for cloudy skies is indeed underestimated by the reanalyses. When considering validations across all sites, the Root Mean Square Differences (RMSD) of the three reanalyses are 6.49%, 6.60%, and 8.65%, respectively. NCEP CFSv2 and ECMWF ERA5 perform notably better than NASA MERRA2. These results are consistent with those of Schmeisser et al. (2018).

However, such a significant underestimation is not seen for clear skies, especially for NCEP CFSv2 and ECMWF ERA5. Under clear skies, these reanalyses even exhibit a slight overestimation of atmospheric absorptivity at many sites. Therefore, by any measure, cloud absorption is still likely to be underestimated by the current reanalyses.

4.3. Difference of cloud absorption anomaly among reanalyses

The results shown in Section 3 demonstrate cloud absorption anomaly may still exist in current model-derived reanalyses. It fluctuates not only with sites but also with reanalyses. The mean cloud absorption modeled by NCEP CFSv2 is approximately half of the observed value, the mean cloud absorption modeled by ECMWF ERA5 is about one-third of the observed value, and the mean cloud absorption modeled by NASA MERRA2 is even less than one-quarter of the observed value. Clearly, cloud absorption anomaly revealed by NCEP CFSv2 or ECMWF ERA5 is much smaller than that of NASA MERRA2.

It is surprising that NCEP CFSv2 is closer to the observation than ECMWF ERA5, given that both models appear to have adopted the same radiative scheme, with even ECMWF ERA5 utilizing a newer implementation of this scheme (Hogan and Bozzo, 2018; Saha et al., 2014). This may be resulted from other factors. After all, in addition to the radiative scheme, theoretically many factors, such as surface albedo, cloud top height, cloud phase, cloud 3D morphology, cloud profile, cloud water path *etc.*, may all impact cloud absorption, although their impacts are indecisive (Li and Trishchenko, 2001).

Nevertheless, this does not imply that NCEP CFSv2 performs better than ECMWF ERA5 in cloud simulation. NCEP CFSv2 in fact significantly overestimates cloudy skies frequency compared to observations and the other two models (Goswami et al., 2017). This may be an important reason why they show the lower cloud absorption anomalies.

4.4. Comparison with previous studies

Compared with previous studies, we find observed R values are noticeably lower than those reported previously.

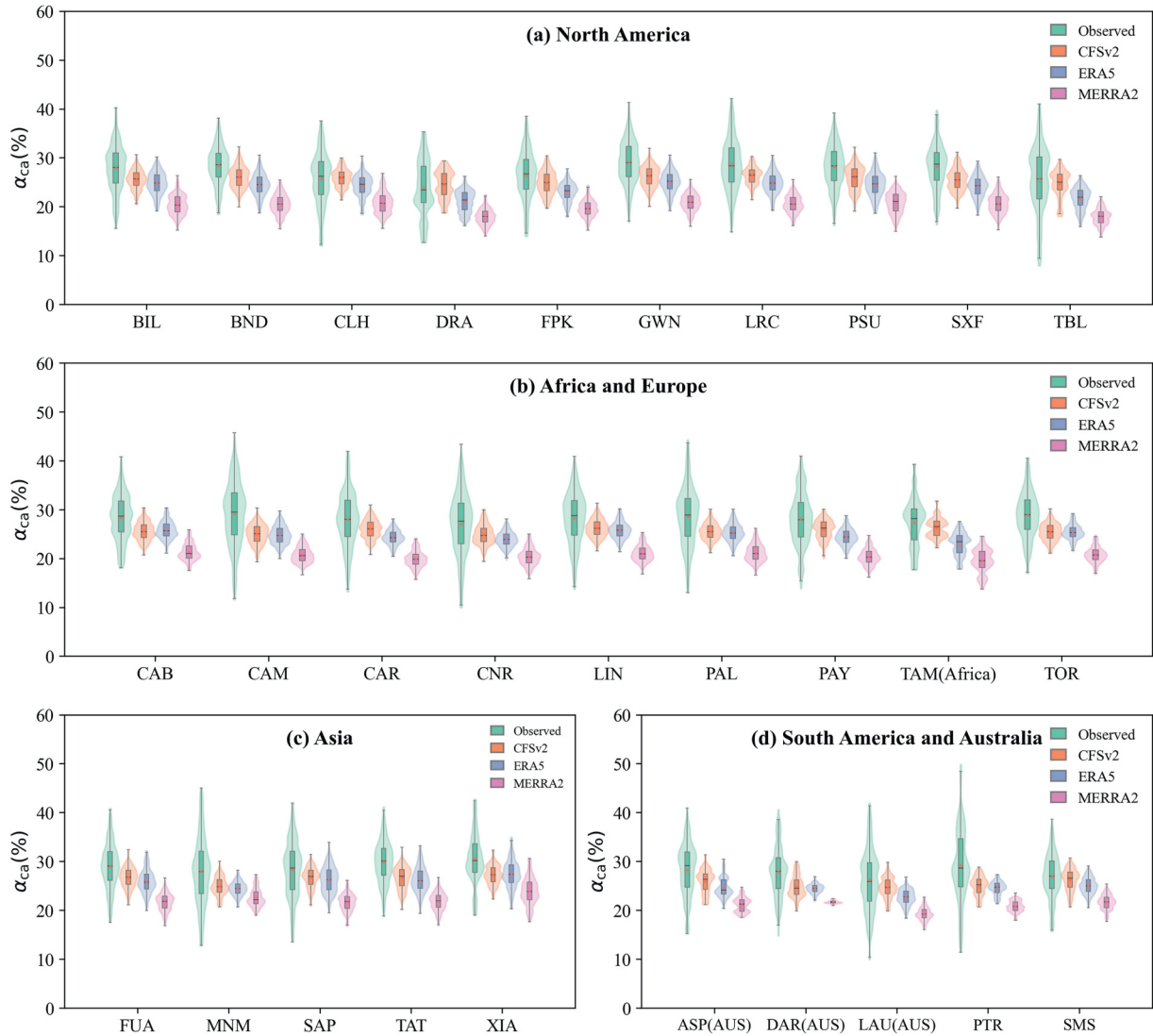


Fig. 7. Box-whisker plots of observed, NECP CFSv2 modeled, ECMWF ERA5 modeled, and NASA MERRA2 modeled cloudy-atmosphere's absorptivity (α_{ca}) across all BSRN and SURFRAD sites (Lines in red, boxes, and whiskers denote the average values, interquartile ranges, and minimum/maximum values, respectively, (a) North America, (b) Africa and Europe, (c) Asia, (d) South America and Australia).

The NASA MERRA2 modeled R values remain as low as those reported in the mid-1990s, however, the modeled R values of NCEP CFSv2 and ECMWF ERA5 far exceed those reported in any previous studies. In other words, the magnitudes of cloud absorption anomalies revealed by the state-of-the-art models are clearly smaller than those reported earlier, particularly for NCEP CFSv2 and ECMWF ERA5.

From the perspective of α_c , NCEP CFSv2, ECMWF ERA5, and NASA MERRA2 on average underestimate cloud absorptivity by approximately 3.09, 4.92, and 5.51 percentage points, respectively. The global diurnally averaged shortwave incident radiation is approximately 341.3 W/m^2 (Stephens et al., 2012). This implies that NCEP CFSv2, ECMWF ERA5 and NASA MERRA2 underestimate globally-mean cloud absorption by approximately 10.54 , 16.79 and 18.80 W/m^2 , respectively. Excessive absorption caused by higher water vapor under cloudy

skies (one limitation from the observation) on average would lead to a 0.67% increase in observed α_c values. If its impact is corrected, the underestimations by NCEP CFSv2, ECMWF ERA5 and NASA MERRA2 are 8.26 , 14.50 and 16.51 W/m^2 , respectively. These underestimations are also remarkably smaller than those (often larger than 20 W/m^2) found by Chen (1997).

The presence of cloud absorption anomaly certainly results in theoretically the overestimation for surface-received solar radiation. Besides numerical models, this phenomenon also regularly appears in the satellite retrieval of surface solar irradiance (Huang et al., 2019). Many retrieving algorithms based on radiative transfer theory (Lu et al., 2023; Tang et al., 2016; Zhang et al., 2014, 2018) demonstrate surface solar irradiance under cloudy skies is notably overestimated comparing against surface measurements. The magnitude of overestimation essentially matches that of anomalous cloud absorption, ranging

approximately between 10 and 30 W/m² (Huang et al., 2019).

5. Conclusions

Using the latest satellite and surface observations and the three state-of-the-art model-derived reanalyses, we again investigate and discuss cloud absorption anomaly, a longstanding issue in the field of cloud–radiation interactions. Our results demonstrate as a whole the modeled cloud absorption from the three reanalyses is still lower than the observed significantly, although there are a few site-specific departures for NECP CFSv2. The NCEP CFSv2 modeled mean cloud absorption is approximately half of the observed value, the ECMWF ERA5 modeled mean cloud absorption is about one-third of the observed, and the NASA MERRA2 modeled value is less than one-quarter of the observed. Meanwhile, under cloudy skies, observed atmospheric absorptivity markedly exceeds the modeled values, whereas under clear skies, they align quite well. The fact that such a systematic discrepancy occurs only under cloudy skies further supports our conclusion that cloud absorption anomalies may still exist.

However, we must note that, compared to previous studies, its magnitude has decreased notably, particularly for NCEP CFSv2 and ECMWF ERA5. At a few sites, the underestimations of NECP CFSv2 are insignificant or even nonexistent. Overall, NECP CFSv2, ECMWF ERA5 and NASA MERRA2 underestimate globally-mean cloud absorption by approximately 10.54, 16.79 and 18.80 W/m², respectively, which is much smaller than the previous reports indicating underestimations often exceeding 20.00 W/m².

In addition, true cloud absorption is very difficult to observe, as clouds naturally mix with aerosols, water vapor, and other atmospheric constituents. To isolate cloud absorption, most studies assume that the absorptions of other atmospheric constituents remain consistent between cloudy and clear skies. This will result in an imperfect cloud absorption observation, which particularly includes excessive water vapor absorption relative to clear skies. If the excessive water vapor absorption is corrected, globally-mean cloud absorption underestimations by NECP CFSv2, ECMWF ERA5 and NASA MERRA2 would be reduced to 8.26, 14.50 and 16.51 W/m², respectively.

Therefore, we can conclude that cloud absorption may be still underestimated by current model-based reanalyses, although the degree of underestimation has decreased substantially. This systematic discrepancy may be a macro and universal phenomenon. It varies with not only across sites but among also specific radiative transfer schemes in models. More advanced radiative transfer schemes may substantially mitigate the so-called ‘cloud absorption anomaly’. Future efforts may still need to focus on improving our understanding of the processes underlying cloud–radiation interactions.

Declaration of competing interest

The authors declare no conflict of interest.

CRedit authorship contribution statement

You-Jing Fu: Writing – review & editing, Writing – original draft, Visualization, Validation, Methodology, Investigation, Formal analysis, Data curation. **Guang-Hui Huang:** Writing – review & editing, Writing – original draft, Visualization, Validation, Supervision, Resources, Project administration, Methodology, Investigation, Funding acquisition, Formal analysis, Conceptualization. **Zi-Yan Huang:** Writing – review & editing, Writing – original draft, Visualization, Validation, Methodology, Investigation, Data curation. **Xu-Feng Wang:** Writing – review & editing, Writing – original draft, Visualization, Validation, Supervision, Conceptualization. **Han Ma:** Writing – review & editing, Validation, Supervision, Resources, Conceptualization. **Guo-Jiang Wang:** Writing – review & editing, Validation, Resources, Data curation. **Chun-Lin Huang:** Writing – review & editing, Validation, Investigation, Conceptualization. **Xiao-Hua Hao:** Writing – review & editing, Validation, Resources, Conceptualization. **Peng-Fei Zhao:** Writing – review & editing, Validation, Investigation.

Acknowledgments

This study is supported by the National Natural Science Foundation of China (42171322 and 42371365) and the Science and Technology Program of Gansu Province (23JRRA1059). We thank the BSRN and SURFRAD communities for their high-quality surface observations, and the CERES and MODIS science teams for their advanced satellite products. We also thank the data support from NCEP CFSv2, ECMWF ERA5, and NASA MERRA2.

Appendix A. Supplementary data

Supplementary data to this article can be found online at <https://doi.org/10.1016/j.accres.2025.10.003>.

References

- Ackerman, A.S., Toon, O.B., 1996. Unrealistic desiccation of marine stratocumulus clouds by enhanced solar absorption. *Nature* 380, 512–515. <https://doi.org/10.1038/380512a0>.
- Ackerman, T.P., Flynn, D.M., Marchand, R.T., 2003. Quantifying the magnitude of anomalous solar absorption. *J. Geophys. Res. Atmos.* 108. <https://doi.org/10.1029/2002jd002674>.
- Arking, A., 1996. Absorption of solar energy in the atmosphere: discrepancy between model and observations. *Science* 273, 779–782. <https://doi.org/10.1126/science.273.5276.779>.
- Asano, S., Uchiyama, A., Yamazaki, A., et al., 2004. Solar radiation budget from the MRI Radiometers for clear and cloudy air columns within arese II. *J. Atmos. Sci.* 61, 3082–3096. <https://doi.org/10.1175/JAS-3288.1>.

- Cess, R.D., Zhang, M.H., Minnis, P., et al., 1995. Absorption of solar radiation by clouds: observations versus models. *Science* 267, 496–499. <https://doi.org/10.1126/science.267.5197.496>.
- Chen, H., 1997. On the anomalous absorption of solar radiation by water clouds and by the cloudy atmosphere. *J. Atmos. Sci.* 21, 750–757. <https://doi.org/10.3878/j.issn.1006-9895.1997.06.13> (Chinese).
- Chou, M.-D., Suarez, M.J., 1999. A solar radiation parameterization for atmospheric studies. <https://ntrs.nasa.gov/citations/19990060930>.
- Crisp, D., 1997. Absorption of sunlight by water vapor in cloudy conditions: a partial explanation for the cloud absorption anomaly. *Geophys. Res. Lett.* 24, 571–574. <https://doi.org/10.1029/97gl50245>.
- Emde, C., Buras-Schnell, R., Kylling, A., et al., 2016. The libradtran software package for radiative transfer calculations (version 2.0.1). *Geosci. Model Dev. (GMD)* 9, 1647–1672. <https://doi.org/10.5194/gmd-9-1647-2016>.
- Fang, Y., Cao, L., 2025. Simulated terrestrial climate and carbon cycle response to cloud albedo enhancement over ocean and land. *Adv. Clim. Change Res.* <https://doi.org/10.1016/j.accre.2025.06.003>.
- Feng, Z., Leong Tan, M., Juneng, L., et al., 2025. Effects of solar radiation modification on precipitation extremes in southeast Asia: insights from the GEOMIP G6 experiments. *Adv. Clim. Change Res.* <https://doi.org/10.1016/j.accre.2025.04.009>.
- Goswami, T., Rao, S.A., Hazra, A., et al., 2017. Assessment of simulation of radiation in NCEP Climate Forecasting System (CFSV2). *Atmos. Res.* 193, 94–106. <https://doi.org/10.1016/j.atmosres.2017.04.013>.
- Haefelin, M., Kato, S., Smith, A.M., et al., 2001. Determination of the thermal offset of the eppley precision spectral pyranometer. *Appl. Opt.* 40, 472–484. <https://doi.org/10.1364/AO.40.000472>.
- Hausfather, Z., Marvel, K., Schmidt, G.A., et al., 2022. Climate simulations: recognize the ‘hot model’ problem. *Nature* 605, 26–29. <https://doi.org/10.1038/d41586-022-01192-2>.
- He, J., Hong, L., Lu, N., et al., 2025. Development of a high-resolution dataset of future monthly surface solar radiation by combining CMIP6 projections and satellite-based retrievals. *Adv. Clim. Change Res.* <https://doi.org/10.1016/j.accre.2025.02.007>.
- Hogan, R.J., Bozzo, A., 2018. A flexible and efficient radiation scheme for the ecwf model. *J. Adv. Model. Earth Syst.* 10, 1990–2008. <https://doi.org/10.1029/2018ms001364>.
- Huang, G., Li, X., Huang, C., et al., 2016. Representativeness errors of point-scale ground-based solar radiation measurements in the validation of remote sensing products. *Remote Sens. Environ.* 181, 198–206. <https://doi.org/10.1016/j.rse.2016.04.001>.
- Huang, G., Li, Z., Li, X., et al., 2019. Estimating surface solar irradiance from satellites: past, present, and future perspectives. *Remote Sens. Environ.* 233. <https://doi.org/10.1016/j.rse.2019.111371>.
- Kiehl, J., Hack, J., Zhang, M., et al., 1995. Sensitivity of a GCM climate to enhanced shortwave cloud absorption. *J. Clim.* 8, 2200–2212. [https://doi.org/10.1175/1520-0442\(1995\)008<2200:SOAGCT>2.0.CO;2](https://doi.org/10.1175/1520-0442(1995)008<2200:SOAGCT>2.0.CO;2).
- Li, Z., Barker, H.W., Moreau, L., 1995. The variable effect of clouds on atmospheric absorption of solar radiation. *Nature* 376, 486–490. <https://doi.org/10.1038/376486a0>.
- Li, Z., Cribb, M.C., Trishchenko, A.P., 2002. Impact of surface inhomogeneity on solar radiative transfer under overcast conditions. *J. Geophys. Res. Atmos.* 107. <https://doi.org/10.1029/2001jd000976>.
- Li, Z., Moreau, L., 1996. Alteration of atmospheric solar absorption by clouds: simulation and observation. *J. Appl. Meteorol. Climatol.* 35, 653–670. [https://doi.org/10.1175/1520-0450\(1996\)035<0653:AOASAB>2.0.CO;2](https://doi.org/10.1175/1520-0450(1996)035<0653:AOASAB>2.0.CO;2).
- Li, Z., Moreau, L., Arking, A., 1997. On solar energy disposition: a perspective from observation and modeling. *Bull. Am. Meteorol. Soc.* 78, 53–70. [https://doi.org/10.1175/1520-0477\(1997\)078<0053:OSE-DAP>2.0.CO;2](https://doi.org/10.1175/1520-0477(1997)078<0053:OSE-DAP>2.0.CO;2).
- Li, Z., Trishchenko, A.P., 2001. Quantifying uncertainties in determining sw cloud radiative forcing and cloud absorption due to variability in atmospheric conditions. *J. Atmos. Sci.* 58, 376–389. [https://doi.org/10.1175/1520-0469\(2001\)058<0376:QUIDSC>2.0.CO;2](https://doi.org/10.1175/1520-0469(2001)058<0376:QUIDSC>2.0.CO;2).
- Lu, Y., Wang, L., Zhou, J., et al., 2023. Assessment of the high-resolution estimations of global and diffuse solar radiation using WRF-solar. *Adv. Clim. Change Res.* 14, 720–731. <https://doi.org/10.1016/j.accre.2023.09.009>.
- McFarlane, S.A., Mather, J.H., Mlawer, E.J., 2016. Arm’s progress on improving atmospheric broadband radiative fluxes and heating rates. *Meteorol. Monogr.* 57, 20.1–20.24. <https://doi.org/10.1175/amsmonographs-d-15-0046.1>.
- Molod, A., Takacs, L., Suarez, M., et al., 2015. Development of the GEOS-5 atmospheric general circulation model: evolution from merra to MERRA2. *Geosci. Model Dev. (GMD)* 8, 1339–1356. <https://doi.org/10.5194/gmd-8-1339-2015>.
- Morcrette, J.J., Barker, H.W., Cole, J.N.S., et al., 2008. Impact of a new radiation package, McRAD, in the ECMWF integrated forecasting system. *Mon. Weather Rev.* 136, 4773–4798. <https://doi.org/10.1175/2008mwr2363.1>.
- Norris, P., Takacs, L.L., Putman, W., et al., 2020. Transition to the rrtmg shortwave radiation code in GEOS models. NASA global model. Assimil. Off. Res. Brief 6. Greenbelt, MD, USA.
- O’Hirok, W., Gautier, C., 2003. Absorption of shortwave radiation in a cloudy atmosphere: observed and theoretical estimates during the second Atmospheric Radiation Measurement Enhanced Shortwave Experiment (ARESE). *J. Geophys. Res. Atmos.* 108. <https://doi.org/10.1029/2002jd002818>.
- Ohmura, A., Dutton, E.G., Forgan, B., et al., 1998. Baseline surface radiation network (BSRN/WCRP): new precision radiometry for climate research. *Bull. Am. Meteorol. Soc.* 79, 2115–2136. [https://doi.org/10.1175/1520-0477\(1998\)079<2115:BSRNBW>2.0.CO;2](https://doi.org/10.1175/1520-0477(1998)079<2115:BSRNBW>2.0.CO;2).
- Pilewskie, P., Valero, F.P., 1995. Direct observations of excess solar absorption by clouds. *Science* 267, 1626–1629. <https://doi.org/10.1126/science.267.5204.1626>.
- Pincus, R., Barker, H.W., Morcrette, J.J., 2003. A fast, flexible, approximate technique for computing radiative transfer in inhomogeneous cloud fields. *J. Geophys. Res. Atmos.* 108. <https://doi.org/10.1029/2002jd003322>.
- Ramanathan, V., Subasilar, B., Zhang, G., et al., 1995. Warm pool heat budget and shortwave cloud forcing: a missing physics? *Science* 267, 499–503. <https://doi.org/10.1126/science.267.5197.499>.
- Ross, A., Willson, V.L., 2018. *Basic and Advanced Statistical Tests: Writing Results Sections and Creating Tables and Figures*. Sense-Publishers, Rotterdam.
- Saha, S., Moorthi, S., Wu, X., et al., 2014. The NCEP climate forecast system version 2. *J. Clim.* 27, 2185–2208. <https://doi.org/10.1175/JCLI-D-12-00823.1>.
- Satheesh, S., Ramanathan, V., 2000. Large differences in tropical aerosol forcing at the top of the atmosphere and Earth’s surface. *Nature* 405, 60–63. <https://doi.org/10.1038/35011039>.
- Schmeisser, L., Hinkelman, L.M., Ackerman, T.P., 2018. Evaluation of radiation and clouds from five reanalysis products in the Northeast Pacific Ocean. *J. Geophys. Res. Atmos.* 123, 7238–7253. <https://doi.org/10.1029/2018jd028805>.
- Stephens, G.L., 1996. How much solar radiation do clouds absorb? *Science* 271, 1131–1133. <https://doi.org/10.1126/science.271.5252.1131>.
- Stephens, G.L., Li, J., Wild, M., et al., 2012. An update on Earth’s energy balance in light of the latest global observations. *Nat. Geosci.* 5, 691–696. <https://doi.org/10.1038/ngeo1580>.
- Stokes, G.M., Schwartz, S.E., 2003. The atmospheric radiation measurement program. *Phys. Today* 56, 38–44. <https://doi.org/10.1063/1.1554135>.
- Su, W., Corbett, J., Eitzen, Z., et al., 2015. Next-generation angular distribution models for top-of-atmosphere radiative flux calculation from ceres instruments: methodology. *Atmos. Meas. Tech.* 8, 611–632. <https://doi.org/10.5194/amt-8-611-2015>.
- Tang, W., Qin, J., Yang, K., et al., 2016. Retrieving high-resolution surface solar radiation with cloud parameters derived by combining modis and mtsat data. *Atmos. Chem. Phys.* 16, 2543–2557. <https://doi.org/10.5194/acp-16-2543-2016>.

- Wiscombe, W.J., 1995. An absorbing mystery. *Nature* 376. <https://doi.org/10.1038/376466a0>.
- Yang, K., Koike, T., Ye, B., 2006. Improving estimation of hourly, daily, and monthly solar radiation by importing global data sets. *Agric. For. Meteorol.* 137, 43–55. <https://doi.org/10.1016/j.agrformet.2006.02.001>.
- Zhang, X., Liang, S., Zhou, G., et al., 2014. Generating global land surface satellite incident shortwave radiation and photosynthetically active radiation products from multiple satellite data. *Remote Sens. Environ.* 152, 318–332. <https://doi.org/10.1016/j.rse.2014.07.003>.
- Zhang, Y., He, T., Liang, S., et al., 2018. Estimation of all-sky instantaneous surface incident shortwave radiation from moderate resolution imaging spectroradiometer data using optimization method. *Remote Sens. Environ.* 209, 468–479. <https://doi.org/10.1016/j.rse.2018.02.052>.
- Zhao, P., Huang, G., Wang, X., et al., 2025. Improving light use efficiency models via the introduction of both the diffuse fraction and radiation scalar. *Sci. Total Environ.* 971, 179065. <https://doi.org/10.1016/j.scitotenv.2025.179065>.